EPJ manuscript No.
(will be inserted by the editor)

Exclusive measurement of quasi-free η-photoproduction from deuterium

J. Weiß[1], P. Achenbach[2], R. Beck[2], V. Hejny[3], V. Kleber[3], M. Kotulla[1], B. Krusche[4], V. Kuhr[5], R. Leukel[2], V. Metag[1], V.M. Olmos de Léon[1], R.O. Owens[6], F. Rambo[5], A. Schmidt[2], U. Siodlaczek[7], H. Ströher[3], F. Wissmann[5], and M. Wolf[1]

[1] II. Physikalisches Institut, Justus-Liebig-Universität Gießen, Heinrich-Buff-Ring 16, D-35392 Gießen
[2] Institut für Kernphysik, Johannes-Gutenberg-Universität Mainz, Johannes-Joachim-Becher-Weg 45, D-55099 Mainz
[3] Institut für Kernphysik, Forschungszentrum Jülich GmbH, D-52425 Jülich
[4] Department für Physik und Astronomie, Universität Basel, Klingelbergstrasse 82, CH-4056 Basel
[5] II. Physikalisches Institut, Georg-August-Universität Göttingen, Bunsenstr. 7-9, D-37073 Göttingen
[6] Department of Physics and Astronomy, University of Glasgow, Glasgow G128QQ, UK
[7] Physikalisches Institut, Eberhard-Karls-Universität Tübingen, Auf der Morgenstelle 14, D-72076 Tübingen

Received: date / Revised version: date

Abstract. Quasi-free photoproduction of η-mesons from the deuteron has been measured at the tagged photon facility of the Mainz microtron MAMI with the photon spectrometer TAPS for incident photon energies from the production threshold at 630 MeV up to 820 MeV. In a fully exclusive measurement η-mesons and recoil nucleons were detected in coincidence. At incident photon energies above the production threshold on the free nucleon, where final state interaction effects are negligible, an almost constant ratio of $\sigma_n/\sigma_p = 0.66 \pm 0.10$ was found. At lower incident photon energies the ratio rises due to re-scattering effects. The average ratio agrees with the value extracted from a comparison of the inclusive $d(\gamma,\eta)X$ cross section to the free proton cross section via a participant - spectator model for the deuteron cross section ($\sigma_n/\sigma_p = 0.67 \pm 0.07$). The angular dependence of the ratio agrees with the expected small deviation of neutron and proton cross section from isotropy due to the influence of the $D_{13}(1520)$ resonance. The energy dependence of the ratio in the excitation energy range of the $S_{11}(1535)$ resonance disfavors model predictions which try to explain this resonance as $K\Sigma$-bound state.

PACS. 13.60.Le Meson production – 25.20.Lj photoproduction reactions

1 Introduction

The first excited state of the nucleon with the quantum numbers $I(J^P) = 1/2(1/2^-)$, the so-called $S_{11}(1535)$ resonance has very interesting properties and its structure was recently intensely debated in the literature [1,2,3,4]. The discussion centered around the unusual large decay branching ratio ($b_\eta \approx 50\%$ [5]) of this resonance into the $N\eta$ channel. The much weaker coupling of the closeby $P_{11}(1440)$ and $D_{13}(1520)$ resonances to the $N\eta$ channel can be explained by simple phase space arguments since they need to decay with relative orbital angular momentum $l = 1, 2$ which is suppressed close to threshold. However, also the second S_{11}-resonance at 1655 MeV has only a branching ratio into $N\eta$ of 1 % or less. Glozmann and Riska [1] have argued, that these decay patterns can be understood as a isospin selection rule in their quark model with quark-diquark clusterization of the nucleon. Their diquark clusters in the nucleon ground state and in the $S_{11}(1535)$ have both $I = 0$ but the diquark cluster in the $S_{11}(1650)$ has $I = 1$. Consequently, the decay via the isoscalar η-meson is strongly suppressed for the second S_{11}. Other work even questioned the very nature of the $S_{11}(1535)$ as a nucleon resonance. Kaiser et al. [2,3] treated the resonance as a quasi-bound $K\Sigma$-state and Bijker et al. [4], failing to explain the $S_{11}(1535)$ properties in their model, suggested a quasi-bound $N\eta$ (penta-quark) state. If such suggestions are correct, the immediate question would be where are the regular low lying three quark states predicted in the quark model with the quantum numbers $1/2^-$,1/2?

The precise experimental determination of the properties of this state is essential in order to resolve the problem. From the experimental point of view the strong coupling to the $N\eta$-channel is advantageous since it allows an almost background free investigation of this resonance. Precise experiments measuring angular distributions [6], the photon beam asymmetry [7] and the target asymmetry [8] for η-photoproduction and the dependence of the electromagnetic helicity coupling on the momentum transfer in η-electroproduction [9] have been recently reported for

Correspondence to: Bernd.Krusche@unibas.ch

the proton. However, photoproduction from the proton alone gives no information about the isospin structure of the electromagnetic excitation of the resonance. It is thus desirable to study the reaction also on the neutron, but due to the non-availability of free neutron targets such experiments must rely on meson photoproduction from light nuclei. Due to its small binding energy and the comparatively well understood nuclear structure the deuteron is the obvious choice as target nucleus.

Previously, quasifree η-photoproduction from the deuteron was measured in two experiments [10,11] carried out at the Mainz MAMI- and Bonn ELSA-accelerators. In the first experiment [10] only the η-mesons were detected via their two-photon decay channel. The neutron - proton cross section ratio was determined from the comparison of the inclusive cross section to the free proton cross section in the framework of a participant - spectator model. In the second experiment [11] recoil protons and neutrons were measured, but the η-mesons were only identified via a missing mass analysis of the recoil nucleons. In the present experiment η-mesons were unambiguously identified in an invariant mass analysis of their decay photons and the recoil nucleons were detected in coincidence. This allows a very clean comparison of the proton and neutron cross sections measured under identical conditions from the nucleons bound in the deuteron. The kinematic over-determination furthermore allows the test of the participant - spectator assumption. At the same time the cross section of the inclusive reaction $d(\gamma,\eta)X$ was re-measured with much higher statistical accuracy.

2 Experimental setup

The experiment was carried out using the Glasgow tagged photon facility [12] installed at the Mainz microtron MAMI [13,14] with the TAPS detector [15,16].

The quasi-monochromatic photon beam covered the energy range from 580 - 820 MeV with a resolution of 1 - 2 MeV and an average photon flux of $\approx$ 250 kHz/MeV. The liquid deuterium target of 10 cm length was mounted in a vacuum chamber of 90 cm diameter, constructed from carbon fiber. The thin wall thickness (4 mm) of the chamber ensured that scattering and energy loss of the recoil nucleons were minimized. The photons from the 2γ-decay of the η-mesons and the recoil nucleons were detected with the electromagnetic calorimeter TAPS. The device consists of 504 BaF_2 crystals and is optimized for the detection of photons via electromagnetic showers but has also excellent particle detection capabilities. Each BaF_2 scintillator module is of hexagonal shape, 25 cm long (corresponding to 12 radiation lengths), and has an inner diameter of 5.9 cm. The modules were arranged in six blocks with 8×8 BaF_2 crystals each, placed at polar angles of $\pm 50^\circ$,$\pm 100^\circ$, and $\pm 150^\circ$ in a plane around the scattering chamber at a distance of 54 cm from the target center. A hexagonally shaped forward wall of 120 crystals was positioned at 0° around the beam pipe at a distance of 1 m from the target. The BaF_2-modules of the blocks were equipped with individually read-out plastic scintillators (NE102) at their front sides for the identification of charged particles. The modules of the forward wall were operated in phoswich mode, i.e. the light from each BaF_2-module and the corresponding plastic scintillator was read out by the same photo-multiplier tube. These modules effectively worked as ΔE-E-telescopes and thus allowed the separate identification of photons, recoil protons and neutrons. A detailed description of the experimental setup is given in [17], where the results for quasifree η-photoproduction from ^4He are reported.

3 Data analysis

The separation of photons from recoil particles was achieved with a time-of-flight measurement with typically 500 ps resolution (FWHM), the pulse-shape discrimination capability of the BaF_2-scintillators, and the charged particle veto detectors. The energies and impact points of the photons were determined in the usual way (see e.g. [17]) from the energies deposited by the electromagnetic showers in clusters of BaF_2 scintillator modules. The energy calibration of the individual modules was done with the help of cosmic radiation. The η-mesons were then identified via their two photon decay, which has a branching ratio of 39.2%, with a standard invariant mass analysis of coincident photon pairs using:

$$m_{\rm inv}^2 = (E_1+E_2)^2-(\mathbf{p}_1+\mathbf{p}_2)^2 = 2E_1E_2(1-\cos\Phi_{12}) \quad (1)$$

where E_i denotes the energies, $\mathbf{p}_i$ the momenta of the two photons and Φ_{12} the relative angle between them (units with $\hbar = c = 1$ are used throughout the paper). An invariant mass resolution for the η of $\approx$ 60 MeV (FWHM) was achieved (see [17]). The data sample with an identified η-meson was used to extract the angular distributions and the total cross section of inclusive η-photoproduction from the deuteron. The energy and angle dependent detection efficiency of the TAPS detector for the 2γ-decay of η-mesons was determined as described in [24,19] with a Monte Carlo simulation using the GEANT code [18]. It is important to note that no model assumptions about the non-trivial energy and angular distributions of the η-mesons in the three body final state were needed for the modeling of the detection efficiency. This is possible because in the investigated energy range the detector has a non-vanishing detection probability for all kinematically possible combinations of the meson lab angle and energy. The absolute normalization of the cross section was obtained in the usual way from the target thickness and the photon flux [24,19].

The recoil nucleons were detected in the forward wall which subtended laboratory angles between 5° and 20°. Due to the Lorentz boost, only a few nucleons were seen in the side-ward blocks which covered lab angles larger than 35°. The recoil protons and neutrons were identified by their pulse shape signature and their time-of-flight (see [17]). The standard energy calibration of TAPS, which is done with cosmic muons, is only valid for photons since the energy response of the BaF_2-plastic phoswich telescopes is

different for particles. Furthermore charged particles like protons undergo some energy loss in the target and the wall of the scattering chamber. The energy information of the protons was re-calibrated using the kinematic overdetermination of the reaction when the η is detected in coincidence with the proton. This is possible because in the energy range of interest $np\eta$ is the only final state with proton and η-meson. In this case the only missing particle is the neutron and the energy of the proton can be varied until the missing mass of the reaction (see below) equals the neutron mass. This correction was not done event-by-event but an average correction as function of the proton energy obtained from the cosmic calibration was determined. Since there is no direct correlation of the energy response of the detector and the kinetic energies of the neutrons, the neutron energies were determined from the time-of-flight measurement. The energy resolution achieved by this procedures can be judged from the missing mass spectra where the mass of the non observed nucleon is derived from the energy of the incident photon and the momenta of the η-meson and the detected nucleon using:

$$\Delta E = (E_d + E_\gamma) - (E_\eta + E_p) \quad (2)$$

$$\Delta \mathbf{p} = \mathbf{p}_\gamma - (\mathbf{p}_\eta + \mathbf{p}_p) \quad (3)$$

$$m^2_{\mathrm{miss}} = \Delta E^2 - \Delta \mathbf{p}^2 \quad (4)$$

where E_d, E_γ, E_η and E_p are the total energies of the incident deuteron and photon and the detected η-meson and participant nucleon and $\mathbf{p}_\gamma$, $\mathbf{p}_\eta$, $\mathbf{p}_p$ are the respective momenta .

The expected value for the missing mass (i.e. proton or neutron mass) is subtracted from m_{miss}, so that the resulting distributions for $\Delta m = m_{miss} - m_N$ peak at zero, which in case of the η-proton coincidence is enforced by the calibration procedure. The result of this analysis is shown in fig. 1. The resolution for the η-neutron coincidence is not as good as for the η-proton coincidence due to the limited time-of-flight resolution (500 ps FWHM, 1 m flight path).

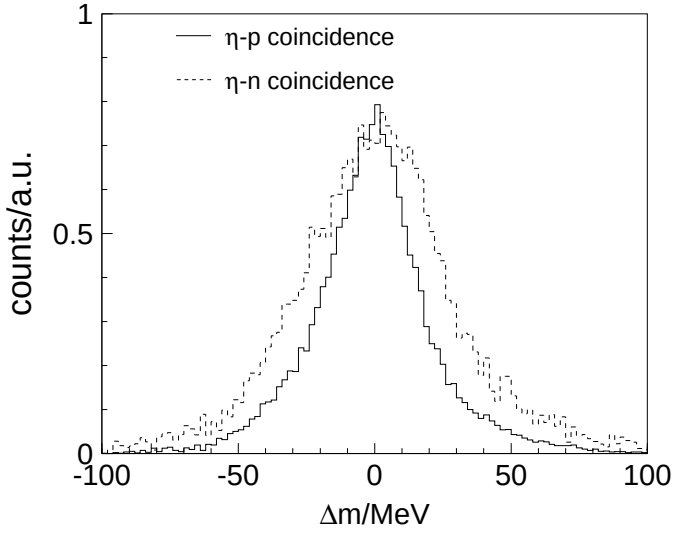

Fig. 1. Missing mass of the coincident η nucleon system. The expected mass value is subtracted.

As discussed above, the detection efficiency of the η-mesons was simulated with the GEANT package, but the simulation of neutron and proton efficiencies is much less precise. The recoil particle detection efficiencies were thus experimentally determined with the help of reactions where the nucleons are 'tagged' by the detection of other reaction products. The reaction $p(\gamma,\pi^0)p$ with the detection of the π^o was used for the proton efficiency and the reaction $p(\gamma,\pi^0\pi^+)n$ with detection of the π^0- and π^+-mesons for the neutron efficiency. In both cases the momentum of the recoil nucleon was determined from the incident photon energy and the measured momenta of the pions and the efficiencies were constructed from the ratios of the event numbers with and without additional detection of the recoil nucleon. The procedure is described in detail in [17].

The acceptance of the TAPS detector for the two-photon decay of η-mesons covers the full polar angular range. However, recoil nucleons were only detected for lab angles between 5° and 20° and recoil protons with kinetic energies below ≈ 60 MeV did not reach the detector. Since an extrapolation to the full angular and energy range of the recoil nucleons would be model dependent, the exclusive cross sections are only given in the TAPS acceptance. This means, that only events with recoil nucleons in the restricted angular and energy ranges were considered (neutrons with energies below the proton detection threshold were removed) and corrected for the TAPS detection efficiencies for η-mesons, neutrons and protons discussed above. In this way, no total exclusive cross sections were obtained, however the cross sections within the TAPS acceptance can be used to extract the neutron - proton cross section ratio. Here one has to keep in mind that due to the Lorentz boost a large fraction of the recoil nucleons is emitted into the angular range covered by the forward wall (see [17]). Furthermore is important, that as shown below, the cross section ratio is not strongly angular dependent and that due to the influence of Fermi motion a modest restriction of the angular range of the recoil nucleons does not restrict the angular range of the coincident η-mesons.

4 Results and discussion

4.1 Inclusive η cross section

Eta-photoproduction from the neutron can be measured via the $d(\gamma,\eta)np$ reaction in so-called quasi-free kinematic where the η-meson is produced on one nucleon, called the participant, while the other nucleon can be regarded as a spectator. The total inclusive cross section for η-photoproduction from the deuteron is shown in fig. 2. The data agrees with our previous result [10], but has much higher statistical quality and extends to somewhat higher incident photon energies so that the resonance position of the S_{11}-state ($W_R \approx 1540$ MeV, $E_\gamma \approx 795$ MeV) is covered. The extraction of the cross section ratio σ_n/σ_p

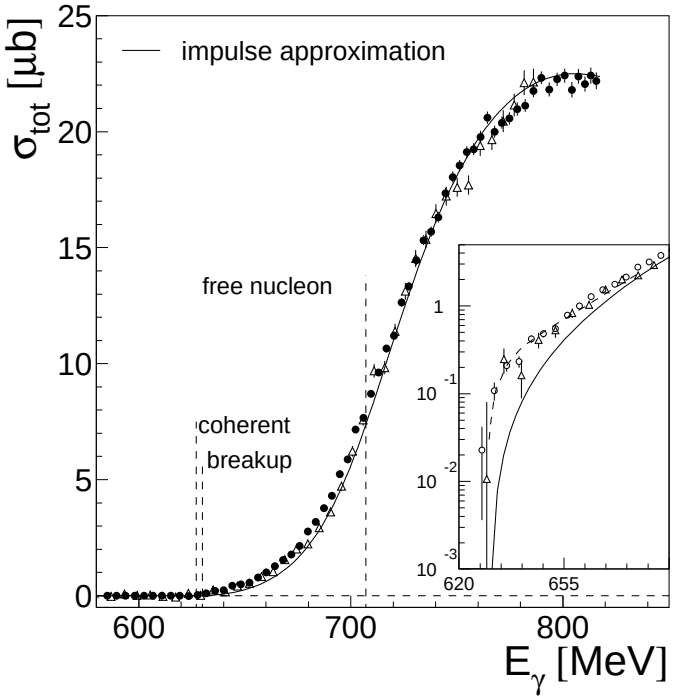

Fig. 2. Inclusive η photoproduction cross section from the deuteron. Circles: present experiment, triangles: ref. [10]. The dashed lines give the deuteron coherent, the deuteron breakup and the free nucleon production thresholds. The solid curve is a fit of the impulse approximation model to the data (see text). Insert: threshold region. The dashed curve is the result of a model including FSI effects [28]
.

from this data relies on the participant - spectator approximation as in [10,17]. A Breit-Wigner curve fitted to the cross section of the $p(\gamma,\eta)p$ reaction was folded with the momentum distribution of the bound nucleons calculated from the deuteron wave function [21]. The result was adjusted to the measured inclusive $d(\gamma,\eta)X$ cross section with a constant factor representing an energy independent σ_n/σ_p ratio. The result of this fit is also shown in fig. 2. At energies above the η-production threshold on the free nucleon the data is very well reproduced with the constant ratio $\sigma_n/\sigma_p = 0.67 \pm 0.005 \pm 0.07$, where the first error is statistical and the second comes from the systematic uncertainties of the proton and deuteron cross sections. At lower incident photon energies the data is underestimated by this fit. This is however expected since it is known [22, 23,24,28] that in this energy range the cross section from the deuteron is enhanced by final state interaction effects. The dashed curve in the insert of fig. 2 shows the result of a calculation with the same ratio of σ_n/σ_p which includes NN- and ηN-FSI effects [28] and is in good agreement with the data.

4.2 The participant spectator model

The extraction of the cross section ratio σ_n/σ_p from inclusive data where only the η-meson is detected, relies on two assumptions. The contribution from the coherent reaction $d(\gamma,\eta)d$ must be negligible, which is true for the deuteron in the energy range of interest [10,11,20]. The other assumption is the validity of the spectator - participant model which is used to extract the cross section ratio from a comparison of the inclusive deuteron data to the cross section on the free proton folded with the momentum distribution of the nucleons bound in the deuteron [10,17]. This means in particular that the cross section from the bound nucleons must not be affected by off-shell effects beyond nuclear Fermi motion and re-scattering contributions must be negligible. Such effects can be much better controlled when the recoil nucleon is detected in coincidence with the η-meson. In this case, one can directly compare the cross section of the bound proton to the bound neutron and furthermore one can select kinematic conditions close to the ideal quasi-free situation.

The lab momentum of the non-detected spectator nucleon was constructed from the measured momenta of the η-meson and the participant nucleon according to eq. 3. The x- and y-components (perpendicular to the photon beam) of the momentum are shown in fig. 3. As expected

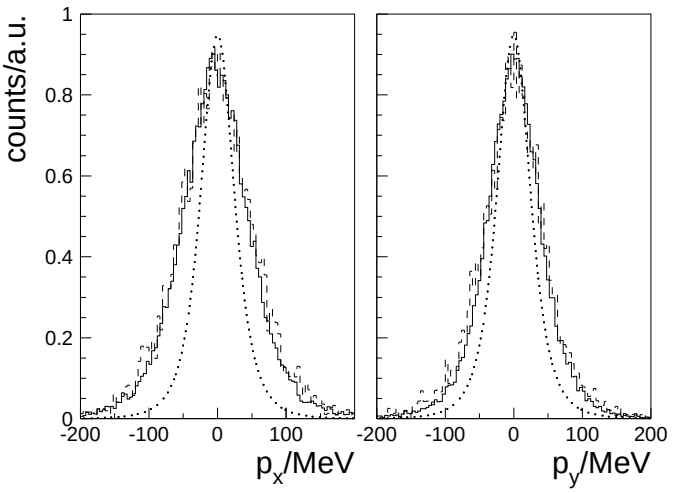

Fig. 3. x (left) and y (right) momentum distributions of reconstructed proton (solid) and neutron (dashed), respectively. Dotted curves: momentum distribution of the bound nucleons calculated from the deuteron wave function without taking resolution effects into account.

the distributions are centered around zero. In the participant - spectator approximation the spectator nucleon picks up the momentum $-\mathbf{p}_F$ where $\mathbf{p}_F$ is the Fermi momentum of the participant nucleon which is symmetrically distributed around zero. The momentum distribution of the bound nucleons calculated from the deuteron wave function [21] is shown for comparison. The difference between the measured distributions and the prediction from

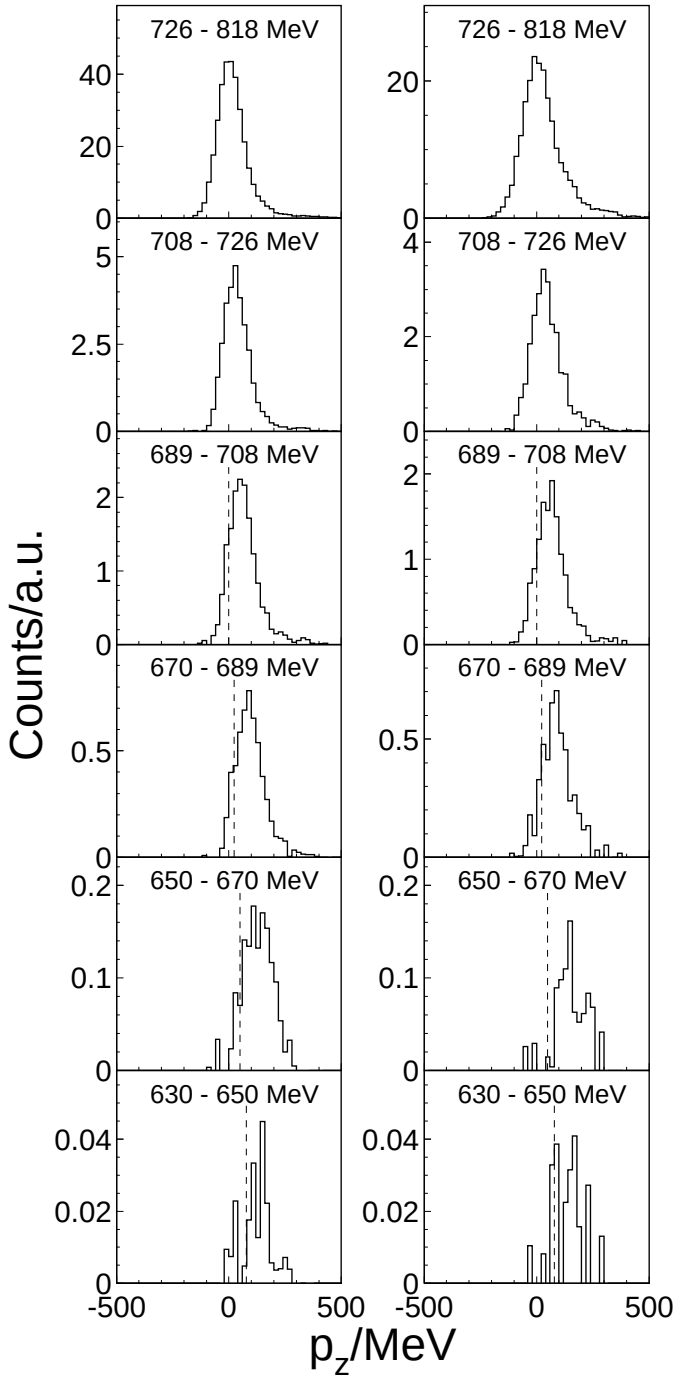

Fig. 4. Reconstructed z-component of the momentum of the spectator nucleon (left: reconstructed proton, i.e. participating neutron, right: reconstructed neutron, i.e. participating proton). Dashed lines give the minimum required momentum to produce the η meson for that particular photon beam energy.

the wave function is mainly due to instrumental resolution effects.

The z-component (parallel to the photon beam) of the spectator nucleons is shown in fig. 4 for different bins of incident photon energy. In this case the distribution is approximately symmetric around zero for high incident photon energies, but the situation changes for low incident photon energies. At energies below the production threshold on the free nucleon ($\approx$ 707 MeV) the reaction is only possible for participant nucleons with a z-component of the Fermi momentum anti-parallel to the photon beam. Consequently, spectator momenta in photon beam direction are selected. Very close to the threshold for coherent η-production from the deuteron ($\approx$ 628 MeV) energy and momentum conservation enforce that spectator and participant nucleon have only a small relative momentum in the final state. This means that for very low incident photon energies no experimental separation of 'participants' and 'spectators' is possible and the probability for final state interaction between the nucleons becomes large so that the participant - spectator approximation breaks down.

In the ideal case where re-scattering effects etc. can be neglected, the measured quasi-free cross sections correspond to the elementary cross sections on the nucleon folded with the momentum distributions of the bound nucleons. However, due to the kinematic over-determination of the exclusive reaction it is also possible to reconstruct event-by-event the total cm energy of the participant nucleon - η system via:

$$s = (E_\eta + E_p)^2 - (\mathbf{p}_\eta + \mathbf{p}_p)^2 \tag{5}$$

and to deduce the effective incident photon energy $E_\gamma^\star$ which would lead to the same $\sqrt{s}$ for an incident nucleon at rest:

$$E_\gamma^\star = \frac{s - m_p^2}{2m_p} \,. \tag{6}$$

In this way it is not only possible to eliminate the Fermi smearing but one can even extract a cross section ratio for values of $\sqrt{s}$ which are larger than $\sqrt{s}$ for a given incident photon energy on a nucleon at rest.

4.3 Neutron-proton cross section ratio

The exclusive cross sections in the TAPS acceptance and the neutron - proton ratio as function of the beam energy are summarized in fig. 5. The ratio over the full range of incident photon energies was obtained with no further cuts on the reaction kinematics. In addition, above the production threshold on the free nucleon a ratio with a cut on the z-component of the spectator nucleon around zero ($\pm 1.5\sigma$ of a Gaussian fitted to the p_z distribution in the highest photon energy bin of 726–818 MeV) is shown in the figure. This cut removes events in which due to large Fermi momenta spectator nucleons have been detected in TAPS and falsely interpreted as participant nucleons. However the effect of the cut is small since at the higher incident photon energies participant and spectator nucleons are well distinguished.

The average of the ratio above the production threshold on the free nucleon is 0.66$\pm$0.01 (statistical error). However, even in this energy range the data seem to show some dependence on the incident photon energy. Taking

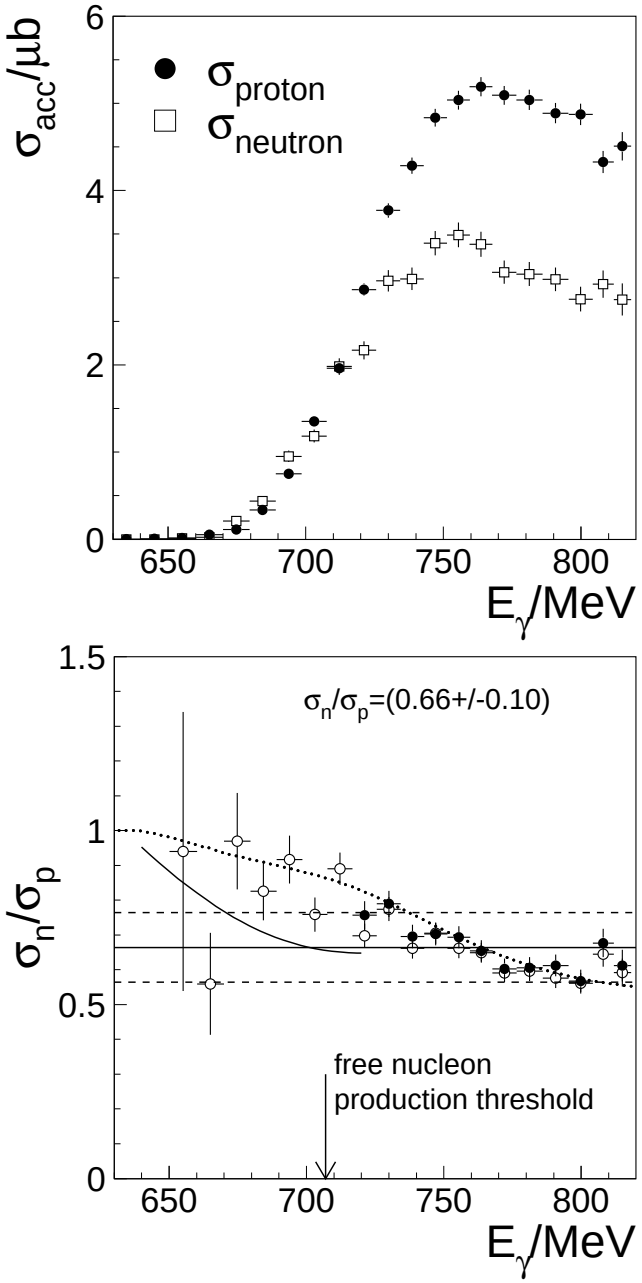

Fig. 5. Upper part: cross section for coincident measurement of η meson and nucleon (the geometrical acceptance for the recoil nucleons is not corrected). Lower part: ratio of σ_n/σ_p without (○) and with (●) cut on z-momentum of reconstructed nucleon to select participant nucleons (see text). The solid line is a calculation of Fix et al. [22]. The dotted line is the ratio of Fermi smeared proton and neutron cross sections corresponding to the neutron - proton ratio as function of equivalent photon energies (see text below).

into account this possible variation a conservative estimate of $\sigma_n/\sigma_p = (0.66 \pm 0.10)$ is derived for photon energies above the free nucleon production threshold.

The cross section ratio rises significantly at lower incident photon energies and approaches unity. Such a behavior was predicted by Fix and Arenhövel [22] with a model calculation which takes into account NN and ηN re-scattering. This rise therefore does not reflect an energy dependence of the elementary cross section ratio but is a pure nuclear effect. Their prediction for a fixed nucleon lab polar angle of 4° is compared to the data in fig. 5. Here one should keep in mind that in the immediate vicinity of the threshold the kinematic separation between spectator and participant nucleons breaks down. This means that very close to threshold the experimentally observed cross section ratio will approach unity in any case.

Inclusive and exclusive total cross section data allow only the extraction of the ratio of the absolute values of $A^n_{1/2}$, $A^p_{1/2}$ but not of the relative sign which is related to the isospin structure of the helicity amplitudes via:

$$|A^p_{1/2}|^2 = |A^{IS}_{1/2} + A^{IV}_{1/2}|^2 \qquad (7)$$
$$|A^n_{1/2}|^2 = |A^{IS}_{1/2} - A^{IV}_{1/2}|^2$$

where $A^{IS}_{1/2}$ denotes the isoscalar and $A^{IV}_{1/2}$ the isovector part of the helicity amplitude for the proton ($A^p_{1/2}$) and the neutron ($A^n_{1/2}$), respectively. Since the ratio of the absolute values is close to 0.8, either the isovector or the isoscalar part must be strongly dominant and the relative sign between $A^n_{1/2}$ and $A^p_{1/2}$ determines which one. This question has been investigated with the help of coherent η-photoproduction from the deuteron [10,11,20]. In this case only the isoscalar amplitude contributes and the observed very small cross sections have been taken as evidence for a dominant isoscalar contribution.

A different possibility to determine the relative sign originates from interference terms in the angular distributions of quasifree η-production from the deuteron. This can be seen in the following way. Due to the strong dominance of the S_{11}-resonance in η-photoproduction, the cross section can be expressed in good approximation by s-wave multipoles and interference terms of the s-wave with other multipoles [6,31] which gives:

$$\begin{aligned}\frac{d\sigma}{d\Omega} = \; & \frac{q^\star_\eta}{k^\star}[E^2_{o^+} - \mathrm{Re}(E^\star_{o^+}(E_{2^-} - 3M_{2^-})) \\ & +2\mathrm{Re}(E^\star_{o^+}(3E_{1^+} + M_{1^+} - M_{1^-}))cos(\Theta^\star) \\ & +3\mathrm{Re}(E^\star_{o^+}(E_{2^-} - 3M_{2^-}))cos^2(\Theta^\star)] \quad . \end{aligned} \qquad (8)$$

It has been shown [6,31], that in the excitation energy range of the $S_{11}(1535)$, the cross section is dominated by the constant term, the *cos*-term is negligible, and the angular dependence results entirely from the cos^2-term. The responsible amplitude $\mathcal{I}$:

$$\mathcal{I} = Re(E^\star_{o^+}(E_{2^-} - 3M_{2^-})) \qquad (9)$$

results from an interference of the S_{11} excitation (E_{o^+}-multipole) with the D_{13} excitation (E_{2-}-, M_{2-}-multipoles) and can be rewritten in terms of helicity elements as:

$$\mathcal{I} \propto \mathrm{Re}(A^\star_{o+}A_{2-}) \; , \qquad (10)$$

in the usual notation. Close to the resonance positions of the S_{11} and the D_{13}, the product of the real parts of the

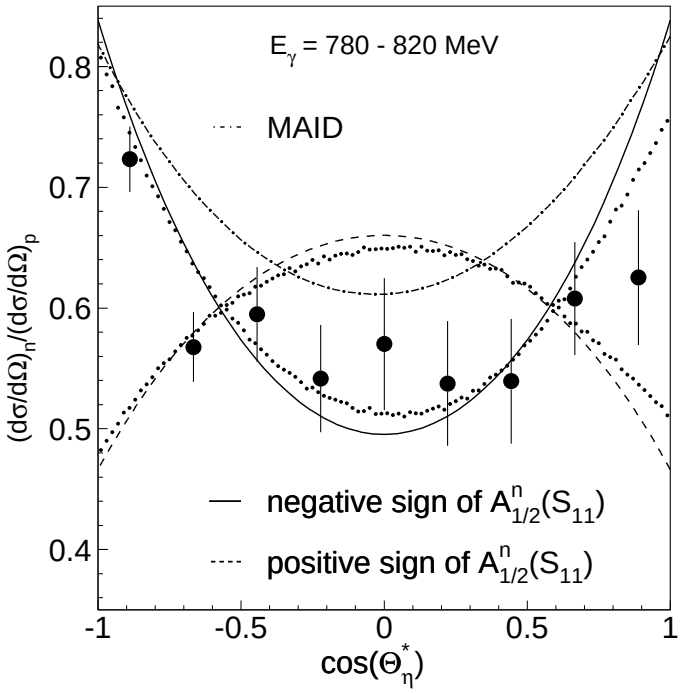

Fig. 6. Neutron - Proton cross section ratio as function of the η cm angle in the excitation energy range of the $S_{11}(1535)$. The dash-dotted curve is the prediction of the MAID-model [30]. The full and dashed lines correspond to the ratio calculated from eq. 13 with negative and positive sign of $A^n_{1/2}$. The two dotted curves show the effect of nuclear Fermi smearing and the detector acceptance on the predicted ratios.

amplitudes is negligible compared to the product of the imaginary parts so that:

$$\mathcal{I} \propto \mathrm{Im}(A_{o+})\mathrm{Im}(A_{2-}) \ . \tag{11}$$

In the vicinity of the two resonances this can be approximated by:

$$\mathcal{I} \propto A^N_{1/2}(S_{11})A^N_{1/2}(D_{13}) \times \mathcal{F}(E_\gamma) \tag{12}$$

where $\mathcal{F}(E_\gamma)$ is the same function for proton and neutron and $A^N_{1/2}$ are the helicity 1/2 couplings for the resonance excitations on proton ($N = p$) and neutron ($N = n$). Therefore the angular distributions can be approximated by:

$$\left(\frac{d\sigma}{d\Omega}\right)_N \propto (A^N_{1/2}(S_{11}))^2 + \mathcal{G}(E_\gamma)A^N_{1/2}(S_{11})A^N_{1/2}(D_{13})(3cos^2(\Theta) - 1) \ . \tag{13}$$

The helicity couplings of the D_{13} resonance are well known from pion photoproduction experiments [5]. We adopt here the results from the latest analysis of the GW-group [25] of $A^p_{1/2}(D_{13})$=(-24±2) (Particle Data Group [5]: -24±9) and $A^n_{1/2}(D_{13})$=(-67±3) (PDG: -59±9). The helicity coupling $A^p_{1/2}(S_{11})$ is taken from [26,30] as (120±20). With these parameters the constant $\mathcal{G}(E_\gamma)$ can be approximated at excitation energies around 800 MeV with eq. 13 from the measured angular distributions of $p(\gamma,\eta)p$ [6] as $\mathcal{G}(800MeV) \approx 0.2$. Since the angular distributions for the proton have a maximum at 90^o [6], $A^p_{1/2}(S_{11})$ is positive, and the helicity couplings for the D_{13} are both negative, we qualitatively expect a minimum at 90^o in the angular distribution of $n(\gamma,\eta)n$ if $A^n_{1/2}(S_{11})$ is negative and a maximum if it is positive.

The angular dependence of the cross section ratio in the excitation region of the S_{11}-resonance is shown in fig. 6 in the cm system of the incident photon and a nucleon at rest. In comparison to the free nucleon case angular distributions of quasifree η-photoproduction from the deuteron are only somewhat smeared out in this frame by Fermi motion [10] as long as the incident photon energies are not to close to the production threshold. Note that due to the influence of Fermi motion, the experiment had non-zero acceptance for all η-emission angles in this frame, although the lab angle of the recoil nucleons was restricted. The data are compared to the ratios predicted from eq. 13 with $A^n_{1/2}(S_{11}) = \pm 93$, corresponding to the observed cross section ratio in this energy region (see fig. 5). As also demonstrated in the figure, the effects of the momentum distribution of the nucleons and the limited acceptance of the detector system have only a small effect on the ratio of the angular distributions. It is obvious that the shape strongly favors the negative sign (reduced χ^2: 1.2 and 8.3 for negative respectively positive sign). The data are also compared to a full calculation with the MAID-model [30], which also reproduces the shape with the negative sign for $A^n_{1/2}(S_{11})$. The small disagreement on the absolute scale between data and MAID corresponds to a slightly different absolute value of the neutron coupling.

4.4 Cross section ratio versus effective photon energy

Due to the momentum distribution of the bound nucleons the exclusive cross section ratios discussed above represent for each incident photon energy an average over a certain range of $\sqrt{s}$ for the photon - nucleon system. This means that when comparing to the elementary cross section ratio predicted by models, one must account for the Fermi smearing which could wash out a possible energy dependence of the ratio. This effect can be eliminated when instead of the incident photon energy the equivalent photon energy $E^\star_\gamma$ (see eq. 6), reconstructed from the over-determined reaction kinematics, is used.

The exclusive cross sections within the TAPS acceptance as function of $E^\star_\gamma$ are shown in fig. 7. The energies of the recoil nucleons, which enter into the calculation of the equivalent photon energy, are measured in different ways (see sec. 3). Consequently, systematic effects due to the resolution and the relative absolute calibration of the recoil nucleon energies must be taken into account for the extraction of the cross section ratio. As discussed in sec. 3 the resolution of the proton recoil energy, determined from the energy deposited in the scintillators, is better than for the neutron recoil energy measured via time-of-flight. In

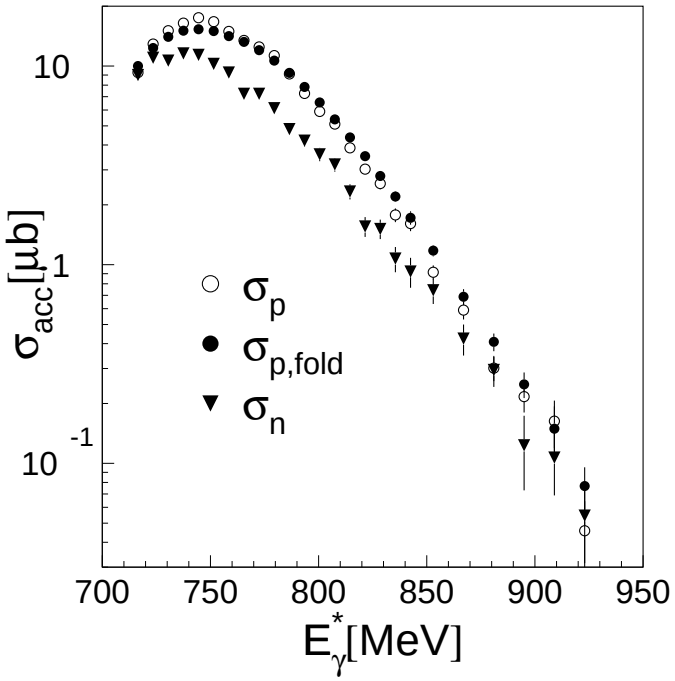

Fig. 7. Exclusive cross sections in the TAPS acceptance of the recoil nucleon as function of the equivalent photon energy. (σ_n: coincident neutron, σ_p: coincident proton, $\sigma_{p,fold}$: proton cross section folded with additional energy smearing).

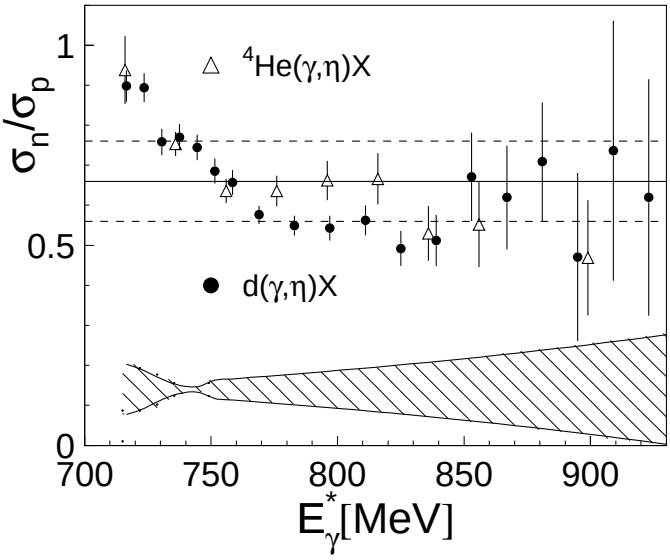

Fig. 8. Ratio of neutron and proton cross section as function of the equivalent photon energy for the deuteron and for ^{4}He [17]. The lines indicate the average extracted from the exclusive cross sections as function of the incident photon energy. The shaded band represents the systematic uncertainty of the ratio due to the relative calibration of the proton and neutron recoil energies.

order to avoid a systematic effect on the cross section ratio, the proton energies were folded with an additional resolution term so that the resolution for the recoil energies of both nucleons became equal. This was controlled via the influence of the resolution on the shape of the missing mass spectra. The folded proton cross section is also shown in the figure, the effect is largest for small photon energies.

The resulting ratio is shown in fig. 8 and compared to the measurement with the ^{4}He target [17] which was now analyzed in the same way. The two data sets show a very similar behavior. Due to the nuclear re-scattering effects the ratios approach unity close to threshold. At higher energies the ratios become almost constant although the deuteron data tend to somewhat lower values around photon energies of 800 MeV, where they are close to the lower limit extracted from fig. 5. This behavior is not inconsistent with the results shown in fig. 5. This is demonstrated with a participant - spectator model calculation using the cross section ratio extracted above from the equivalent photon energy. The result for the cross section ratio as function of the incident photon energy (dotted line in fig. 5) agrees very well with the measured values. On the other hand, the cross section ratio as function of the equivalent photon energy has an additional systematic uncertainty from the relative calibration of the nucleon recoil energies which can give rise to a shift of $E^\star_\gamma$ between protons and neutrons. The possible size of this effect is indicated as shaded band in fig. 8. It was determined in the following way: the energies were artificially changed until a significant shift of the peak positions in the missing mass spectra was observed. Subsequently the cross section ratio was re-analyzed with the modified energy calibration. The uncertainty is almost negligible around 740 MeV, where the two cross section peak, but becomes large in the regions with a steep slope.

5 Conclusions

Inclusive and exclusive η-photoproduction from deuterium has been measured. An impulse approximation model fitted to the inclusive data yields a ratio $\sigma_n/\sigma_p = 0.67 \pm 0.07$ in agreement with an earlier measurement [10].

Fully exclusive data from the deuteron, i.e. the coincident detection of the η-meson *and* the recoil nucleon has been obtained for the first time. The kinematics is overdetermined for this reaction, which allows the reconstruction of the momentum of the spectator nucleon and of $\sqrt{s}$ of the photon - participant nucleon system. The exclusive data was analyzed in two ways: as function of the incident photon energy and as function of the equivalent photon energy corresponding to the reconstructed $\sqrt{s}$. The data are compared to the results from a similar experiment using a ^{4}He target and to model predictions in fig. 9.

The observed rise of the cross section ratio to unity at the breakup threshold for incident photon energies, respectively at the free nucleon threshold for equivalent photon energies is understood. It is a pure nuclear effect due to rescattering contributions etc., which are not related to the behavior of the elementary cross sections on the free nucleon. Therefore the extreme threshold region should not be included into the determination of the neutron - proton ratio for the excitation of the $S_{11}(1535)$ resonance. The

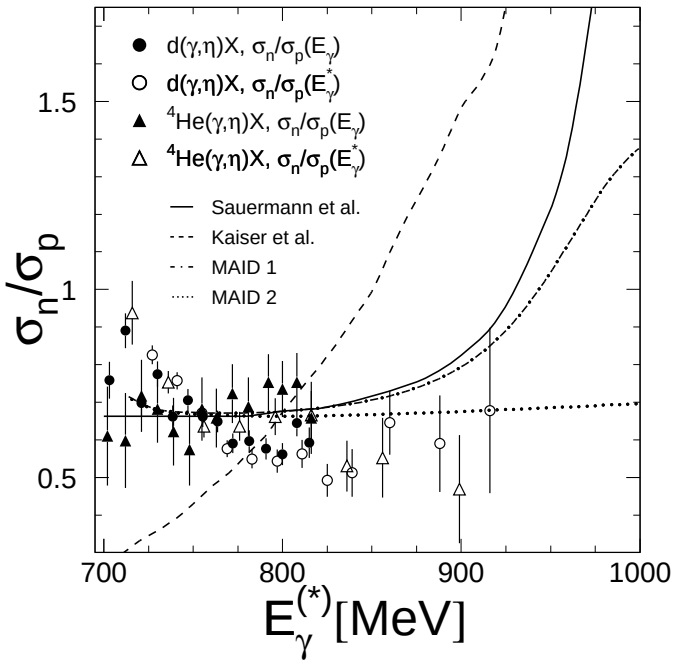

Fig. 9. Ratio of exclusive proton and neutron cross sections in the TAPS acceptance. The deuteron data are compared to the ^4He-data [17] and to model predictions from Sauermann et al. [29] and Kaiser et al. [3]. The curves labeled MAID [30] are the predictions from the full MAID model (MAID1) and a truncated version restricted to the $S_{11}(1535)$-resonance, Born terms and vector meson exchange (MAID2).

ratios are almost constant for higher incident photon energies and the small residual energy dependence is opposite for the deuteron data (slight decrease to higher energies) and the ^{4}He data [17] (slight increase). As a function of the equivalent photon energy the ratios from both measurements show a slight decrease towards higher energies in the excitation energy range of the S_{11}, which lies, however, within the systematic uncertainty of the data. Consequently, no final conclusion can be drawn as to whether a small energy dependence of the elementary cross section ratio for η-photoproduction on the free neutron and proton exists in the excitation energy range of the S_{11}. A comparison of the energy dependence in the S_{11} range to model predictions (see fig. 9) clearly disfavors the interpretation of the resonance as a $K\Sigma$ bound state [2,3]. This model reproduced the cross section for $p(\gamma,\eta)p$ quite well, but predicts a strong rise of σ_n/σ_p, which is not observed.

The cross section ratios derived from the inclusive and exclusive data for *incident* photon energies in the S_{11}-range are compared below to previous results:

$$\begin{aligned}\sigma_n/\sigma_p &= (0.67\pm0.07),\ ^2\text{H},\ \eta \text{ detected; this work} \\ &= (0.66\pm0.10),\ ^2\text{H},\ \eta \textit{ and} \text{ recoil nucleon; this work} \\ &= (0.66\pm0.07),\ ^2\text{H},\ \eta \text{ detected; [10]} \\ &= (0.68\pm0.06),\ ^2\text{H, recoil nucleon detected; [11]} \\ &= (0.67\pm0.07),\ ^4\text{He},\ \eta \text{ detected; [17]} \\ &= (0.68\pm0.09),\ ^4\text{He},\ \eta \textit{ and} \text{ recoil nucleon; [17]}\end{aligned} \tag{14}$$

The values obtained from effective photon energies around the S_{11} position ($E^\star_\gamma$=750 - 850 MeV, see fig. 8) are close to the lower limits of the above results, but have much larger errors due to the systematic uncertainty of the relative energy calibration:

$$\begin{aligned}\sigma_n/\sigma_p(E^\star_\gamma) &= (0.58\pm0.20),\ ^2\text{H, this work} \\ &= (0.62\pm0.20),\ ^4\text{He, this work}\ .\end{aligned} \tag{15}$$

The results from all measurements agree and their uncertainties are dominated by systematic effects like the absolute cross section normalizations and the model dependence of the extraction from inclusive data. This systematic uncertainties are largely independent since the experiments include different target nuclei, different extraction methods of the ratio, and different experimental setups, so that an overall average of the results is meaningful:

$$\langle\sigma_n/\sigma_p\rangle = (0.67\pm0.03) \tag{16}$$

$$|A^n_{1/2}|/|A^p_{1/2}| = (0.819\pm0.018) \tag{17}$$

$$A^{IV}_{1/2}/A^{IS}_{1/2} = (10.0\pm0.7) \tag{18}$$

$$A^{IS}_{1/2}/A^p_{1/2} = (0.09\pm0.01)$$

Inclusion or not of the less precise results obtained from the analysis of the effective photon energies (eq. 15) leaves the overall result unchanged. This precise value of the cross section ratio can then be used for the extraction of the ratio of the electromagnetic helicity couplings $A^n_{1/2}$ and $A^p_{1/2}$ for the excitation of the $S_{11}(1535)$ resonance on the neutron and the proton. Here it is assumed that in the energy range of interest η-photoproduction is so strongly dominated by the excitation of the S_{11} resonance that the sum of all other contributions can be safely neglected [26]. The extraction of the isospin structure of the helicity amplitude, i.e. the ratio $A^{IV}_{1/2}/A^{IS}_{1/2}$ or $A^{IS}_{1/2}/A^p_{1/2}$ furthermore requires the knowledge of the relative phase between the proton and the neutron amplitude. The results from coherent η-photoproduction from the deuteron [11,20] and the behavior of the ratio of the angular distributions for quasifree η-production from the proton and the neutron investigated here, have shown, that the reaction on the nucleon must be dominantly isovector. Under this assumption a 9% isoscalar contribution to the proton amplitude is determined. The lowest value for the proton - neutron ratio in the S_{11} range is 0.55 for equivalent photon energies around 800 MeV in the present experiment. Even if we use this value, the isoscalar component would only rise to 13%. As discussed in [20] such a small isoscalar amplitude is not in agreement with models reproducing the measured coherent cross section which require an isoscalar admixture of roughly 20%. The origin of this discrepancy is not yet understood. It was however recently suggested by Ritz and Arenhövel [27] that the proton and neutron amplitudes could have an unexpected large *complex* relative phase. In this case the amplitude ratio $|A^n_{1/2}|/|A^p_{1/2}| = (0.819\pm0.018)$ could be consistent with a 20% isoscalar admixture.

At higher photon energies a rise of the neutro-proton ratio is predicted by models. This is shown in fig. 9. The full curve is a prediction from a coupled channel model by Sauermann et al. [29]. The dash-dotted and dotted curves are predictions from the MAID model [30] for the full model and for a truncated model which only takes into account the excitation of the $S_{11}(1535)$ resonance, Born terms and vector meson exchange. The predicted rise at the higher photon energies is assigned to the excitation of higher lying nucleon resonances. The measured cross section ratio does not yet show any rise to higher energies, but it is evident that higher incident photon energies must be used to test this prediction.

Acknowledgments

We wish to acknowledge the outstanding support of the accelerator group of MAMI, as well as many other scientists and technicians of the Institut für Kernphysik at the University of Mainz. Stimulating discussions with A. Arenhövel and A. Fix are gratefully acknowledged. This work was supported by Deutsche Forschungsgemeinschaft (SFB 201), the UK Engineering and Physical Science Research Council and the Swiss National Science Foundation.

References

1. L.Y. Glozmann and D.O. Riska, Phys. Lett. **B366** (1996) 305.
2. N. Kaiser et al., Phys. Lett. **B366** (1995) 23.
3. N. Kaiser et al., Nucl. Phys. **A612** (1997) 297.
4. R. Bijker et al., Phys. Rev. **D55** (1997) 2862.
5. D.E. Groom et al. (The Review of Particle Physics), Eur. Phys. J. **A15** (2000) 1
6. B. Krusche et al., Phys. Rev. Lett. **74** (1995) 3736.
7. J. Ajaka et al., Phys. Rev. Lett. **81** (1998) 1797.
8. A. Bock et al., Phys. Rev. Lett. **81** (1998) 534.
9. R. Thompson et al., Phys. Rev. Lett. **86** (2001) 1702.
10. B. Krusche et al., Phys. Lett. **B358** (1995) 40.
11. P. Hoffmann-Rothe et al., Phys. Rev. Lett. **78** (1997) 4697.
12. I. Anthony et al., Nucl. Instr. Meth.**A301** (1991) 230.
13. Th. Walcher, Prog. Part. Nucl. Phys. **24** (1990) 189.
14. J. Ahrens et al., Nuclear Physics News **4** (1994) 5.
15. R. Novotny, IEEE Trans. Nucl. Sci. **38** (1991) 379.
16. A.R. Gabler et al., Nucl. Inst. and Meth. **A346** (1994) 168.
17. V. Hejny et al., Eur. Phys. J. **A6** (2000) 83.
18. R. Brun et al., GEANT, Cern/DD/ee/84-1, 1986.
19. B. Krusche et al., Eur. Phys. J. **A6** (1999) 309.
20. J. Weiß et al., Eur. Phys. J. **A11** (2001) 371.
21. M. Lacombe et al., Phys. Lett. **B101** (1981) 139.
22. A. Fix and H. Arenhövel, Z. Phys. **A359** (1997) 427.
23. A. Sibirtsev et al., Phys. Rev. **C64** (2001) 024006.
24. V. Hejny et al., Eur. Phys. J. **A13** (2002) 493.
25. R.A. Arndt, W.J. Briscoe, I.I. Strakovski, R.L. Workman, nucl-th/0205067.
26. B. Krusche et al., Phys. Lett. **B397** 171.
27. F. Ritz, H. Arenhövel, Phys. Rev. **C64** (2001) 034005.
28. A. Sibirtsev et al., Phys. Rev. **C65** 2002 004007.
29. C. Sauermann, B.L.Friman, W. Nörenberg., Phys. Lett. **B341** (1995) 261; C. Sauermann PhD thesis, TH Darmstadt (1996), unpublished.
30. W.-T. Chiang, S.-N. Yang, L. Tiator, D. Drechsel, Nucl. Phys. **A** 700 (2002) 429. http://www.kph.uni-mainz.de/MAID/maid.html.
31. L. Tiator, D. Drechsel, and G. Knöchlein, Phys. Rev. **C60** (1999) 035210.